Searching for a Reliable Orientation of Ligands in Their Binding Site: Comparison between a Structure-Based (Glide) and a Ligand-Based (FIGO) Approach in the Case Study of PDE4 Inhibitors†

Paola Gratteri, Claudia Bonaccini,* and Fabrizio Melani

Department of Pharmaceutical Sciences, University of Florence, via U. Schiff 6, 50019 Sesto Fiorentino, Firenze, Italy

Received August 31, 2004

Two 3D QSAR Grid/Golpe models, differing in the alignment criterion of the studied phosphodiesterase 4 (PDE4) inhibitors, were compared. The docking-guided alignment, obtained by exploiting the known 3D structure of the PDE4, was used to test and validate the field-fit alignment solution proposed by FIGO procedure. The analysis of the direct (docking) and indirect (FIGO) superposition methodologies occurs through the comparison of the respective PLS coefficient maps. The inclusion in the FIGO algorithm of factors related to the hydrophobicity and shape of the molecules leads to promising results, making the new FIGO algorithm a valid alternative in the molecule overlay, particularly when the 3D structure of the target is unknown.

Introduction

Most drugs act via specific binding to macromolecules such as enzymes, receptors, glycoproteins, and nucleic acids. The most important factors for a favorable interaction between a drug and its specific biological target, most often a protein, are the 3D-complementarity in molecular shape, the formation of hydrogen bonds between functional groups, the formation of hydrophobic interactions between lipophilic surfaces, and van der Waals interactions in stabilizing associated structures. The knowledge of the 3D structure of both ligands and biological targets, or better of the ligand−target complexes, plays a key role in the rational design of new ligands with improved binding affinities, allowing the so-called *receptor-based drug design*. Despite the continuous progress made in the field of biomacromolecular structure determination, the 3D structure of most biological targets is still not known (i.e. membrane spanning GPCRs, ion channels or membrane transporters), although many studies have been devoted to determining at least 3D homology-built models. However, the level of sequence homology between the modeled protein and its template influences the reliability of the model itself, as the structure-based drug design is influenced by the resolution of the 3D structure of the macromolecule. Yet the investigation of the forces involved in the ligand−target interactions for therapeutically relevant proteins of unknown 3D structure is not less important than that of proteins whose 3D structure has been determined. Lacking this knowledge, one possible approach is ligand-based drug design, whereby virtual maps of the structural properties of the binding site are obtained using the information from a set of ligands that share a common binding mode and have an affinity toward the target protein of 3−5 orders of magnitude. A major difficulty in this indirect approach is the need to assume how ligands bind to their target since the quality of the obtained model critically depends on this hypothesis. Many attempts have been made to develop automatic procedures that make it possible to avoid or objectively deal with molecular alignment. Recently, we have set up a computational procedure, FIGO[1] (Field Interaction and Geometrical Overlap), for the 3D alignment of structures. It consists of a field-fit based method whereby the alignment of the molecules occurs via Simplex optimization through the superposition of both molecular interaction fields (MIFs) precalculated with Grid[2] program for a set of compounds, and the heavy atoms (no hydrogen) of their chemical skeleton. A typical FIGO procedure involves the calculation of MIFs using hydrogen-bond acceptor and donor probes. To enhance the description of features depending on hydrophobicity and shape of the molecules, we have improved the FIGO procedure by adding and selecting MIFs from hydrophobic probes according to both their energy values and the distances between them.

Starting from a set of PDE4 inhibitors selected from literature (Table 1),[3−17] this work presents an application of the implemented FIGO procedure and compares its results with those obtained from a docking-guided alignment through the comparison of PLS coefficient plots of the derived Grid/Golpe 3D QSAR models.

Phosphodiesterases (PDEs) constitute a large and divergent family of enzymes responsible for the hydrolysis of second messengers cAMP and cGMP to the correspondent 5′-nucleotide metabolites. PDEs have been classified into 11 isoenzyme types on the basis of structural, biochemical and pharmacological differences. Within each PDE type, further diversity is introduced by alternative splicing of the encoding genes and post-translational modifications of their protein products.[18] PDE type 4 (PDE4) is represented by four gene products (A−D) which themselves give rise to different splicing variants. This PDE class has been characterized by the specific binding of cAMP and the selective inhibition by rolipram. PDE4s are highly expressed in inflammatory

* To whom correspondence should be addressed: Phone: +39-055-4573702, Fax: +39-055-4573671, E-mail: paola.gratteri@unifi.it.

† Preliminary results have been presented at the Genome-Based Drug Design International Conference, March 22−27, 2004, Florence, Italy.

10.1021/jm049289b CCC: $30.25
Published on Web 02/12/2005

Table 1. PDE4 Inhibition Values of the Dataset Compounds[a]

code	compd[b]	pIC_{50}	ref	code	compd[b]	pIC_{50}	ref	code	compd[b]	pIC_{50}	ref	code	compd[b]	pIC_{50}	ref
aa	***4***	*6.284*	3	ah	**9**	7.149	6	nn	***12***	*7.229*	10	sn	**1**	7.276	11
	5	5.785			**10**	6.987			**13**	7.523			**5d**	6.879	
	8	7.092			**11**	5.169			**14**	7.244			***5f***	*7.42*	
	9	6.523			***12***	*7.092*			**15**	6.815			**5i**	6.618	
	10	6.854			***13***	*8.699*			**17**	7.409			**5j**	6.879	
	11	5.848		aj	***1aR***	*7.62*	7		***24***	*6.73*			**5k**	7.432	
	12	6.886			***1aS***	*5.364*			**29**	8.000			**5l**	7.319	
	13	*6.796*			**1bR**	7.553			**30**	7.721			**5m**	7.032	
	14	4.693			**1bS**	6.22			**31**	7.523			***5p***	*7.854*	
	15	5.712			***2a***	*6.604*		ou	**10a**	4.979	13		**6**	6.883	
	17	6.174			**2bR**	6.65			**10d**	4.967		tn	**6a**	7.523	12
	18	6.387			**2bS**	4.481			**10e**	6.569			***6b***	*8.699*	
ac	**6**	6.319	4		***2cR***	*5.879*			**11a**	5.328			**6e**	7.292	
	7	5.432			***2cS***	*4.441*			***11b***	*6.000*			**6f**	7.553	
	8	5.770			***10***	*5.783*			**11e**	6.699			**6g**	7.602	
	9	5.921			***15***	*5.754*			**12a**	5.208			**6h**	7.523	
	10	5.469		ak	roli	6.523	8		***12e***	*6.523*			***6i***	*7.921*	
	11	*5.444*			**4**	6.71			**13b**	5.886			***6j***	*7.678*	
	12	*5.149*			**5**	7.284			**13e**	6.301			**6k**	6.947	
ad	*CDP840*	*6.174*	5		**10**	7.357			**14b**	6.523			**6l**	7.143	
	rp734	8.046			***12***	6.276			**14e**	7.398			**6m**	7.444	
	sb207	6.770			**13**	5.971			**14f**	7.097			**6p**	7.071	
	11	5.785			**14**	5.467			**14g**	6.699		vu	**11d**	6.854	14
	14	6.796			***17***	*6.131*			**14h**	7.046			***11e***	*7.18*	
	15	5.219			**19**	6.921			**16c**	5.770			**11f**	6.638	
	16	6.310			**21**	5.921			**16e**	6.699		wu	**2a**	6.319	15
	17	5.967			**24**	6.495			**17a**	5.26			**2b**	6.538	
	18	5.650			**26**	6.469			**17b**	5.585			**2d**	6.921	
	19	6.569			***28***	*7.097*			**17c**	5.796			**3a**	5.721	
	20	6.051			***30***	*5.602*			**17e**	7.000			**3b**	6.959	
	21	*7.469*			**32**	5.928			***18b***	*6.155*			**3c**	6.77	
	22	6.357		am	**3a**	8.796	9		***18c***	*5.569*		xu	**4a**	7.056	16
	23	7.319			**3c**	7.569			**18e**	6.699			**4b**	6.155	
	24	6.824			***3d***	*7.77*			***18f***	*6.699*			**4c**	6.678	
	26	4.804			***3e***	*8.618*			**19a**	4.790			**4d**	7.292	
	27	4.071			***3f***	*8.42*			**19e**	6.155			**4e**	7.367	
	28	4.072			**3g**	6.114			***20e***	*6.161*			**4f**	6.357	
	29	*7.201*			**4**	6.481			**9a**	4.688			**4h**	6.678	
	30	*6.18*			***5***	*6.495*			**9b**	5.959		zu	***1***	*5.398*	17
	31	7.409			**6a**	8.201			**9c**	5.357			**5**	4	
	32	5.785			***6b***	*6.921*			***9e***	*6.301*			***7***	*6.187*	
	33	*6.796*			**6c**	6.058			***9f***	*5.854*			**8**	6.149	
	34	6.377			**6d**	6.345			***9h***	*6.155*			***13***	*6.387*	
					6e	*6.785*							**14**	5.903	
					6f	7.268							**15**	5.745	
					6g	*7.07*							***16***	*5.939*	
													17	6.119	
													19	6.018	
													20	6.201	

[a] Italic entries represent molecules in the training set. [b] Compound numbering refers to the original article.

cells and in airway smooth muscle; thus, the selective inhibition of PDE4 has been suggested as an interesting target for the development of an alternative therapeutic approach for respiratory diseases such as asthma and chronic obstructive pulmonary disease (COPD).[19]

Recently the crystallographic structure of PDE4 isoenzyme has been solved[20] and made available on the PDB database,[21] enabling the first visual inspection of the PDE4 catalytic site and providing binding and specificity information useful for the drug discovery processes, as well as opening up a series of structural studies on the entire PDE family.

All PDE4 structures nowadays deposited in PDB, either alone (**1f0j**)[20] or cocrystallized with ligands (the inhibitor zardaverine in **1mkd**,[22] the selective inhibitor rolipram in **1q9m**,[23] the product of the catalyzed reaction 5′-AMP in **1ptw**,[24] the nonselective inhibitor IBMX in **1rko**[25]), possess at least two metal cations in the active site. Such cations have been postulated to be involved both in structure stabilization and in the mechanism of catalysis, although the exact nature of the physiological ions is not yet clear, or if they are the same in different PDE4 subtypes. One of them (Me1) coordinates residues from three different domains, thus supporting the idea of a structural role for this metal. Me2 instead seems to be coordinated with the enzyme through only one direct interaction with a protein residue and five water-bridges. Moreover, one of these water molecules (or its hydroxylic-activated form) seems to be involved in the hypothesized catalytic mechanism acting as nucleophile in the hydrolysis of the phopshodiesteric bond of cAMP.[24]

It is clear that many factors contribute to the stabilization of molecular interactions within the PDE active site, and especially in those cases where there is structural information about the protein counterpart, the ligand-based approach can be very useful in highlighting "hidden" interactions. The results presented here indicate that in cases where poor information about protein−ligand interactions are available, the use of

both direct and indirect approaches can produce a more complete scenario for rational drug design.

Results and Discussion

Starting from a set of about 180 PDE4 inhibitors belonging to different chemical classes (Table 1),[3−17] subsets of 60 and 25 compounds (training set, TrS; and test set, TS, respectively) were selected. Care was taken to ensure that the distribution of the biological activity values of the training and test set molecules was representative of the overall dataset.

FIGO Alignment. FIGO[1] represents a Simplex/experimental design-based computational procedure for superposing small ligand molecules to one or more (hyper template, HT) reference structures. In this case study, the product of PDE4-catalyzed reaction, 5′-AMP, and the well-known PDE4 specific inhibitor rolipram were selected as HT. Studies on conformational preferences of cyclic nucleotides demonstrated that the PDE4 substrate cAMP adopts, as global minimum, an anti conformation similar both to the crystal structure of cAMP[26] and to the bound conformation of the recently solved 5′-AMP.[24] This consideration supported the choice of using 5′-AMP bound conformation as part of our FIGO reference structure. As far as the inhibitor rolipram is concerned, computer graphics studies performed by Marivet et al.[27] identified its active conformation as the one with the carbonyl group in the anti orientation, toward the *m*-alkoxy substituent. Recently available crystallographic data partially confirm this assumption showing that rolipram could interact with the binding site both in the anti and in the syn conformation.[28] To clarify this aspect, we aligned, using the FIGO procedure, both conformations of rolipram with the one previously described for 5′-AMP. The obtained results showed that both the syn and the anti conformations align their dialkoxyphenyl moiety similarly with respect to the adenine portion of 5′-AMP, thus differing only in the orientation of the pyrrolidinone ring that in both cases overlays the sugar−phosphate portion of 5′-AMP. This is in agreement with crystallographic data[28] and supports the use of any rolipram conformer as part of HT. Thus all the molecules of the TrS and TS were aligned using the superposed 5′-AMP and rolipram in their bound conformations as HT and using the implemented FIGO algorithm with MIFs also from the hydrophobic (C3) probe. In fact, as was initially formulated, the FIGO algorithm did not explicitly consider the shape of ligands, a feature which is well recognized to be critical for the ligand binding. The addition of the molecular-shape field related to van der Waals and hydrophobic interactions allows good definition of the spatial extension of compounds and appropriate consideration of the shape and dimension of ligands as a main factor for a favorable interaction with their specific biological targets. The use of the shape field appeared particularly suitable in the PDE4 inhibitor study due to the presence in the binding site of wide zones of hydrophobic nature.

Docking Study. Analysis of the Binding Site. A valid docking study requires a preliminary characterization of the binding site with attention to the structural elements critical to the establishment of protein−ligand interactions such as the shape and size of the active site, the ligand accessible zone, the presence of functional water molecules or cofactors, and the flexibility of the protein side chains involved in the ligand−target complex formation.

All the studies regarding the binding site characterization were performed on **1f0j** (the enzyme alone) while experiments of docking and docking accuracy were carried out with **1q9m** (the enzyme in complex with the inhibitor rolipram) taken as the representative structure of the enzyme complexed with ligands.

Characterization of the active-site of **1f0j** was performed by means of program Grid[2]. Grid allows the study of a target, either macromolecules or small molecules such as ligands, and the identification of favorable interaction areas that the target establishes with different probes resembling the chemical features of the interacting counterpart. The probes are moved along the intersection points (nodes) of a grid within which the target is placed. The result is a functional map that highlights the most favorable interaction points between the target and the probes.

With regard to the analysis of structural water molecules, the computation of Grid maps using the water probe (OH2) allows comparison between favorable interaction contours and the actual position of water molecules in the crystal structure of **1f0j** (Figure 1).

The widest interaction area was found in the metal cations zone, where X-rays actually indicate the presence of some coordinating water molecules. This observation confirms that they could really play an active role in the binding of other entities such as metal ions. To clarify the role of these water molecules (H_2O) in the ligand binding, docking experiments were performed which resulted in the worst scores when all the previously examined H_2O were considered. Only two H_2O molecules did not exhibit negative influence on the ligand binding (molecules 1 and 2 in Figure 1 detail). For this reason they were considered for the subsequent calculations.

With regard to the nature of the metal ions Me1 and Me2 of the PDE4 catalytic site, we referred to the existing literature,[20,29,30] considering them as Zn^{2+} (Me1) and Mg^{2+} (Me2), respectively. In fact, while Grid maps computed using both MG2+ and ZN2+ probes agree in identifying the position of Me1 (Figure 2), the computations fail to detect any favorable interaction with the probe in correspondence with Me2.

This result is not supported by experimental data, since the diffraction maps obtained for all the crystallized PDEs to date clearly show two distinct signals attributable to two metal cations. The failure of Grid calculation to detect the Me2 site is probably due to the particular hydration state of this second metal cation, which is difficult to accurately parametrize in a "one-atom" probe.

Because of the implications of protein flexibility in ligand docking strategies, a particular feature of program Grid (directive MOVE) was employed to explore the flexibility of **1f0j**. Two different Grid maps for the OH2 probe were computed, the first setting MOVE=0 (rigid protein) and the second allowing the side chains flexibility (MOVE=1). The differences between the two maps indicate the most flexible regions of the enzyme. Together with some lipophilic amino acids (Leu303,

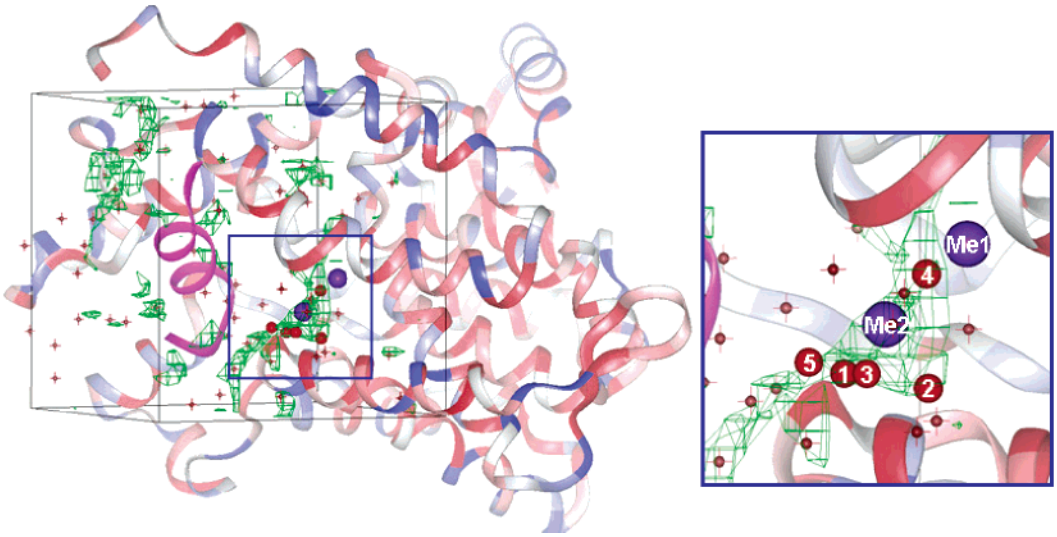

Figure 1. Ribbon diagram of PDE4 color coded for hydrophobicity, except for the 496−508 fragment which is shown in magenta. The grid used for the characterization of the binding site is indicated by black lines. The water molecules present in the crystal structure are reported as red crosses. Green areas represent regions where program Grid estimates a strong interaction energy between the PDE4 and the water probe. The region clearly encompasses the experimental position of water molecules (red balls) indicated by Xu et al.[20] as coordinating the metal ions Me1 and Me2 (purple spheres). On the right is the detail of the binding site. Water molecule 4 is involved in the catalytic mechanism (H2O 748 as in ref 20). Molecules 1 and 2 have been retained in the docking studies (H2O 5 and 19 as in ref 20).

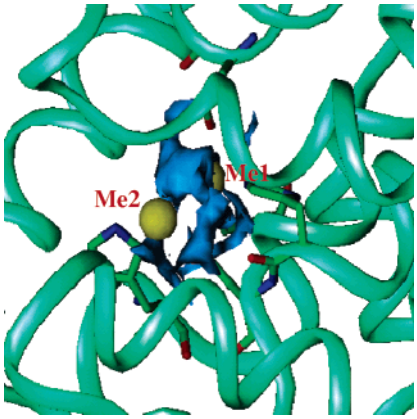

Figure 2. Favorable regions of interaction between MG+2 probe and the active site of **1f0j**. Probe ZN2+, not shown, gives rise to the same results.

Met347, Leu393, Met411, Met431, Val439, Gln443, Ile447, Ile450, Val451), the C-terminal portion of the enzyme represents the most flexible region, as we could expect from the higher B-factor associated with the atoms of this part of the protein. At this level in fact, the structure lacks 6 amino acids (residue 490−495) and even the spatial position of the C-terminal 13-amino acid fragment (residues 496−508) is not assigned with certainty. The catalytic center area, which is formed by the most conserved amino acid residues among the whole PDE family, is not flexible at all.

On the basis of the results obtained from the binding site analysis, the protein formed by the residues 153−486 (corresponding to 79−412 of **1q9m**), two water molecules and Zn^{2+} and Mg^{2+} as metal ions were used for the docking studies. We will refer for further discussions to **1q9m** residue numbering.

Docking Accuracy. The reliability of the docking program Glide[31] used in this study was verified evaluating its performances in reproducing the geometry of bound PDE4 inhibitors taken from all available cocrystallized complexes. This set includes zardaverine (**1mkd**),[22] rolipram (**1q9m**),[23] 5′-AMP (**1ptw**),[24] and IBMX (**1rko**),[25] both in their native and in any conformationally optimized geometries. The docking poses obtained for these ligands have an RMSD for the heavy atom of 2 Å or less from the original PDB coordinates.

Reproduction of the bound zardaverine geometry (**1mkd**) deserves in-depth comment. When Xu et al.[20] crystallized the first structure of PDE4B, they observed a third metal ion, Me3, located at 2.6 Å from the metal center. The data collected for Me3 were consistent with an arsenate (As) ion opportunistically inserted in the crystallization buffer to mimic the phosphate group of the substrate. The position of Me3 confirms the presence of a phosphate binding site near the metal center region. Crystallizing the first ligand−protein structure (**1mkd**), Lee et al.[22] reproduced the same experimental conditions as Xu et al., introducing sodium cacodylate in the crystallization buffer. This resulted in the presence of a dimethylarsenate ion located approximately in the same position as found in **1f0j**, thus influencing the position assumed by the ligand zardaverine in the binding site. Docking accuracy studies on zardaverine were performed both in the presence and absence of a phosphate ion mimicking the arsenate ion (Figure 3). The choice of phosphate is justified assuming that this ion is more realistic than arsenate since the group is present in the enzyme substrate (cAMP). Obviously, as shown in Figure 3, the bound geometry of zardaverine can be reproduced only in the presence of the phosphate ion.

The selective inhibitor rolipram was also docked both in the presence and absence of the phosphate ion; in this case the docked pose of rolipram is not affected by the presence of the phosphate since the bound conformation of the ligand in **1q9m** does not interact with the metal center region. Nevertheless, a paper has recently been published describing a new solved structure of a complex between PDE4B and rolipram,[28] whose 3D

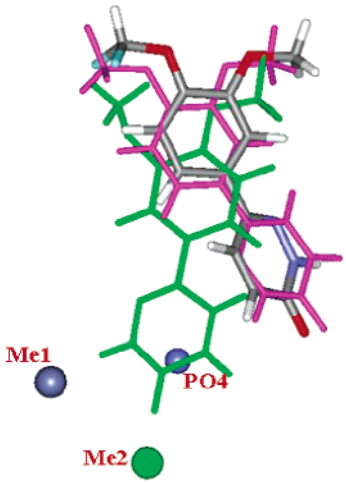

Figure 3. Results of docking accuracy for zardaverine. The crystal orientation of the inhibitor is colored according to atom type. Green and magenta orientations correspond to the Glide docking poses in absence and presence of a phosphate ion (PO4), respectively. Me1 and Me2 refer to the metal cations of the PDE4 binding site.

coordinates were not yet available on PDB when the paper was written. In this case, the authors describe a second orientation (M in ref 28) which locates the pyrrolidinone oxygen of rolipram toward the metal center, in the same position as the phosphate binding site. This observation tends to exclude the hypothesis formulated by Lee et al. of a mechanism of PDE4 inhibitor interaction mediated by a phosphate-type entity, thus supporting our choice in excluding it in further studies.

In the case of **1rko**, reproduction of the bound geometry of the inhibitor IBMX was possible only by adding to the protein used for the docking studies another water molecule. In fact, the structure solved by X-ray shows a water-bridged interaction between the ligand and the Asn321 residue. Only in the presence of this water molecule, which however does not correspond to any favorable interaction areas in our Grid analysis, the docking calculation reproduces the actual orientation of IBMX. However, in recently solved complexes of IBMX with PDE5[25] and PDE3[32] this water molecule has not been observed. For these reasons, and with the lack of selectivity of IBMX toward PDE subtypes in mind, we did not consider the presence of this water molecule in further experiments.

The results discussed up to now have confirmed the reliability of our docking protocol for the study of PDE4 interactions, proving its ability to manage and give due consideration to non protein elements present in the binding site during the ligand-protein interactions.

Glide Alignment. All molecules of the training and test sets were flexibly docked to the PDE4 binding site crystal structure. For each class of inhibitors, program Glide found realistic solutions with good values of the scoring function (either Emodel or Gscore, see Experimental Section), except for diazepinoindoles derivatives (code ou and zu, Table 1) for which a penalty, specifically regarding the lipophilic contact term of the Emodel score function, was assigned. This suggests that diazepinoindoles derivatives are too large to fit well in the known-to-date PDE4 binding site. It must be noted that all the PDE4 structures available on PDB database are complexed with smaller inhibitors with respect to diazepinoindoles and that the present version of Glide does not allow flexibility of the protein at all. The interaction between PDE4 and bulkier molecules could require a conformational adaptation of the binding site which cannot be included in our docking simulations. Another possibility arises from the observation that the available crystal structures of the enzyme are not complete (see the Analysis of the Binding Site section) and that other parts of the protein which have not yet been solved in their three-dimensional structure could take part in the binding of this class of ligands. Based on the docking results, it was decided to exclude ou and zu molecules in the post-Glide model but more in-depth work is in progress on this topic.

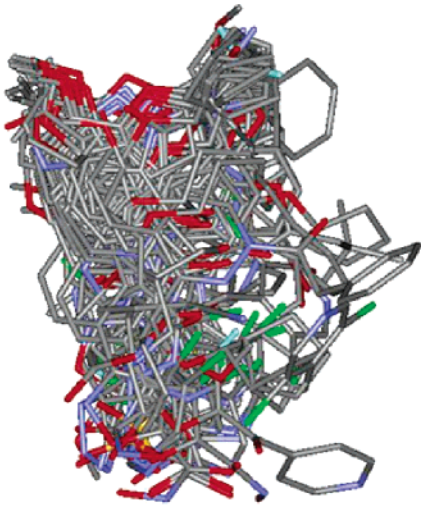

Figure 4. Docking-guided alignment of the training set molecules.

Application of the docking Glide protocol[31] on the TrS inhibitors produced the alignment of the studied molecules (Figure 4).

3D QSAR Models on Phosphodiesterase4 Inhibitors. 3D-QSAR models according to both the FIGO and Glide alignment of TrS molecules were obtained applying the Grid/Golpe procedure. Program Grid[2] was used to generate molecular descriptors (MIFs) that characterize the studied compounds and Golpe,[33] a statistical and data handling program, was used for multivariate regression analysis. MIFs of the PDE4 inhibitors were computed with proper molecular probes (namely DRY, C3, N1, and O probes) in order to resemble the functional groups of amino acids constituting the binding site of PDE4 and to reflect different types of interactions with the target.

Advanced pretreatment and the SRD/FFD (Smart Region Definition, Fractional Factorial Design) variable selection procedure within Golpe were applied and PLS models correlating the biological activities of PDE4 inhibitors with the MIFs were built using the four selected probes. Due to the elimination of the repulsive (positive) interactions (max. cutoff = 0 kcal, see the Experimental Section), only negative values of MIFs, corresponding to attractive, favorable interactions are present in our models. Thus, areas containing negative PLS coefficients correspond to zones in the binding site where energetically favorable interactions produce an increase in the activity.

Figure 5. FIGO-guided alignment of the training set molecules. The surface of the hypertemplate, formed by 5′-AMP (magenta) and rolipram (green), is also shown.

In both post-FIGO and post-Glide models, the DRY probe provides almost the same information as the C3 probe; nevertheless it has been included in the model derivation since it accounts for the overall aromaticity of the PDE4 inhibitors. PLS coefficient maps of both models were compared with each other and with chemical and geometric properties of the PDE4 binding site.

Post-FIGO Model. Comparing the PLS coefficient maps resulting from the Grid/Golpe analysis ($r^2 = 0.991$ $q^2_{LOO} = 0.788$, $q^2_{RG} = 0.396$, $q^2_{ext} = 0.622$), derived according to the FIGO alignment of the TrS molecules (Figure 5) with the chemical and geometrical features of the binding site, yields interesting observations.

Depending on the nature of the probe used (C3, O, and N1), Figure 6A−C highlights the PLS contours corresponding to the position of amino acids of the same features as the probe. Residues corresponding to negative PLS coefficient areas could be considered as the optimal counterparts for the establishment of favorable interactions with ligands.

In Figure 6A (C3 probe), PLS coefficient areas are distributed all over the binding site due to the overall hydrophobicity of PDE4 inhibitors used in this study. However, the wider negative areas are mostly located in correspondence with residues such as Asn321, Pro322, Trp332, Ile336, Met337, Phe340, Met357, Gln369, Phe372. These residues form two hydrophobic sub pockets with different steric tolerance which are able to accommodate ligand functional groups of different dimensions such as the cyclopentyloxy and methoxy groups of the well-known PDE4 inhibitor rolipram.[23] van der Waals interactions also occur with Phe372 where the docked ligands always display $\pi-\pi$ stacking with the aromatic ring of the amino acid residue.

In Figure 6B (O probe) negative coefficient PLS areas are located near Tyr159, Asn321, and Gln369, indicating that interactions at this level, mainly of polar nature, could contribute to the stabilization of protein−ligand complexes. This is in agreement with the involvement of the Asn321 residue in the formation of one hydrogen bond with the adenine ring of 5′-AMP.[24] The observation that this residue is not always conserved in the various PDE isoforms[28] supports the idea of its active role both in substrates and inhibitor selective binding.

Finally, PLS coefficient areas for N1 probe (Figure 6C) highlight many residues as potential donor groups involved in H-bond formation with ligands. Among them, the most important is Gln369, which is one of the amino acids conserved in all the PDE subtypes and it has been observed to interact both with inhibitors[22,23,25] and with the substrate.[24] Moreover, the recently solved crystal structures of PDE3[32] and PDE5,[25] which are characterized by different substrate selectivity with respect to PDE4, show that a possible mechanism for the selectivity could involve the orientation of the Gln369 side chain, which depends on a H-bond network with the neighbor residues[32] that varies from one PDE subtype to another.

Post-Glide Model. PLS coefficient maps of the Grid/Golpe model ($r^2 = 0.891$ $q^2_{LOO} = 0.665$, $q^2_{RG} = 0.660$, $q^2_{ext} = 0.740$), derived according to docking-guided alignment of the TrS molecules (Figure 4), are in good agreement with the position of amino acid residues in the binding site (Figure 7A−C) and with interaction areas found with FIGO approach and discussed above.

As expected, the PLS coefficient plots from the post-FIGO model are generally wider than the post-Glide contours. This is due to the flexibility of the ligands during the docking process which allows subtle conformational adjustment for optimizing the interactions with the target and consequently provides a closer alignment of ligands with respect to the FIGO process.

Moreover, the comparison of the PLS coefficient plots from the two models shows clear differences with regard to the presence of negative contours in the post-FIGO model located in a well defined region, specifically in proximity of the opening of the binding site, as highlighted in Figure 6. This is probably because of the presence in the post-FIGO model of ou and zu derivatives which were excluded in the docking-guided one. Indeed, PLS coefficient contours (not shown) related to the model carried out without ou and zu derivatives (postFIGO*, $r^2 = 0.984$ $q^2_{LOO} = 0.787$, $q^2_{RG} = 0.719$, $q^2_{ext} = 0.653$) do not show these additional interaction areas as in the postGlide model. Nevertheless, the two post-FIGO models exhibit almost the same predictive ability (q^2_{ext}), thus indicating that the quality of the model is not affected by the presence/absence of ou and zu ligands. This consideration, together with the observed difficulty in placing these molecules with the docking protocol, would suggest a different binding mode for diazepinoindole derivatives with respect to the substrate and to the "classical" inhibitors such as rolipram. It can be speculated that the interaction of some classes of ligands involves another domain of PDE4, not present in the available crystal structures, located in the region where Xu et al.[20] have placed the fragment 496−508 and which correspond to the areas pointed out by FIGO. As a further support of this hypothesis, the recently solved complex of PDE4B with rolipram[28] shows an uninterpretable electron density diffraction map in this region.

To summarize, it is not to be excluded that other portions of the enzyme, which are different from the currently available structures, take part in the interaction between PDE4 and ligands; in this hypothesis it could also be possible that some classes of inhibitors (e.g. diazepinoindoles) interact with PDE4 differently than

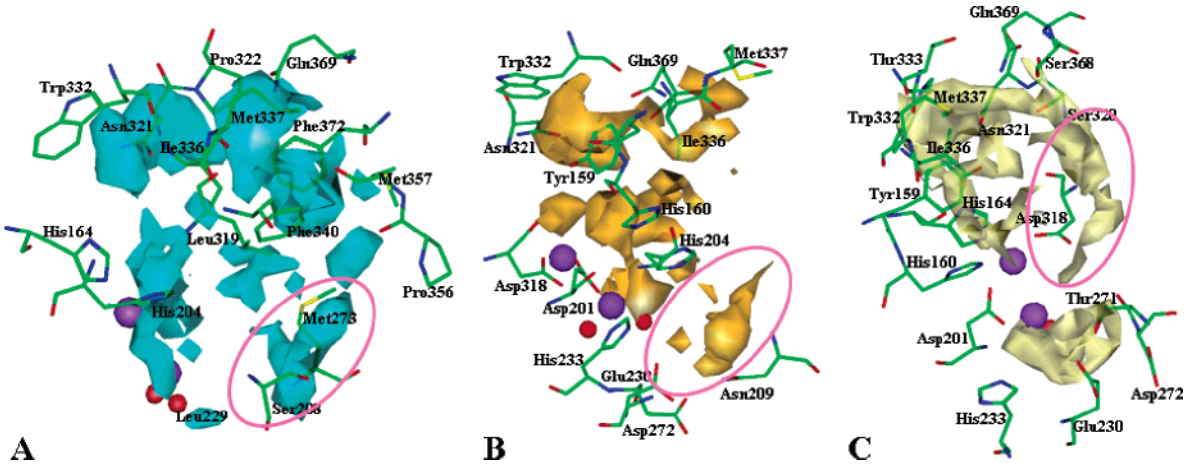

Figure 6. Post-FIGO model comparison between PLS coefficient maps for C3 (A, cyano), O (B, orange), and N1 (C, yellow) probes, contoured at − 0.0013, and the amino acid residues of the enzyme binding site. Only negative coefficients, corresponding to zones in the binding site where energetically favorable interactions produce an increase in the activity, are shown. The indicated interaction areas may correspond to an unsolved portion of the enzyme involved in the binding with inhibitors.

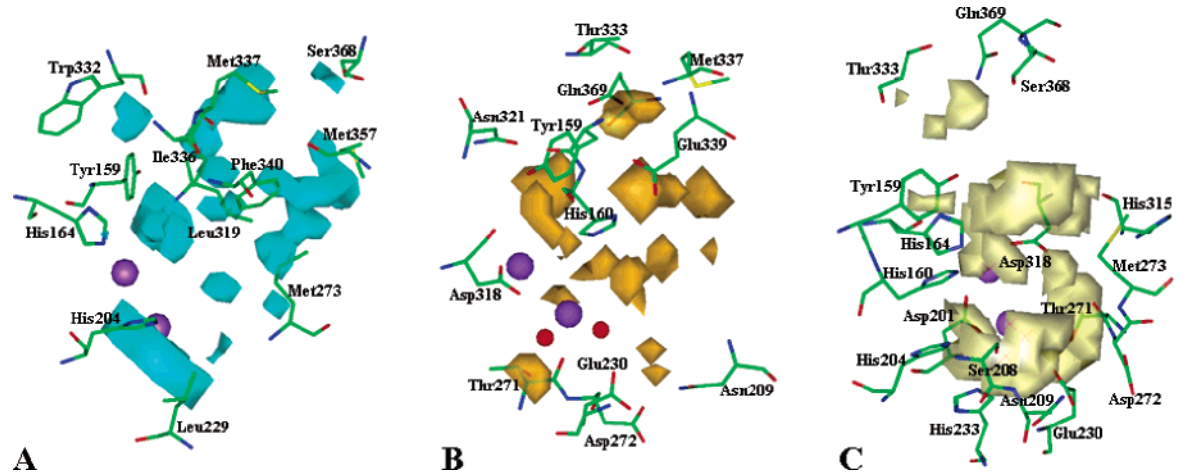

Figure 7. Post-Glide model comparison between PLS coefficient maps for C3 (A, cyano), O (B, orange), and N1 (C, yellow) probes, contoured at −0.0003, and the amino acid residues of the enzyme binding site. Only negative coefficients, corresponding to zones in the binding site where energetically favorable interactions produce an increase in the activity, are shown.

what has been observed to date, but it cannot be predicted for lack of additional structural information.

Conclusion

The availability of the 3D structure of the catalytic site of the phosphodiesterase 4 (PDE4) enzyme together with the use of a set of PDE4 inhibitors belonging to different chemical classes has made it possible to perform a comparative analysis on the alignment modes obtained with two (direct and indirect) approaches and to compare the two virtual binding sites with the corresponding area of the actual 3D structure of the enzyme. The results obtained with the docking-guided alignment of the ligands and with the FIGO field-fit superposition procedure are very promising: many areas of the two resulting virtual receptor sites correspond and match with amino acid residues of the actual binding site. Moreover, the indirect approach has been successful in highlighting interaction areas not revealed by the direct approach. The results obtained appear as an important confirmation of the ability of the FIGO procedure in reproducing reciprocal orientation of molecules to be used in 3D QSAR analysis. This encourages the use of the FIGO procedure in all those situations where the structural information about the target is absent or poor.

Experimental Section

All molecular modeling and QSAR studies were performed on a SGI O2 R10000 workstation.

The structures of all studied compounds were generated using fragment libraries and/or the Builder module of the InsightII2000 package.[34] The energies of the molecules were minimized with conjugate gradient procedure using cvff force field (FF) and the Discover module of InsightII 2000. The biological activity of the compounds was homogeneously expressed as IC_{50} and transformed to the ($-\log IC_{50}$) values for use in the QSAR analysis. TrS and TS compounds were collected according to statistical molecular design principles carried out in the space of the principal component scores of the Volsurf[35] descriptors so that the resulting subsets actually provide an adequate coverage of the whole structural space.

The conformational search was performed using a simulated annealing (SA) procedure which was started using cvff FF, distant dependent dielectric constant, and a convergence criterion of 0.001 kcalmol^{-1}Å^{-1}. The molecular dynamic (MD) simulation took 1000 fs to reach 900 K. The system was then kept at 900 K for 2000 fs and subsequently cooled to 400 K, at regular intervals, by decreasing the simulation temperature. Molecules were then allowed to minimize in order to reach the final minimum conformation. The described cycle was

repeated 100 times so that 100 energy-minimized conformers for each PDE4 inhibitor were obtained. The output of the conformational search procedure was submitted to a cluster analysis obtaining subsets of conformers for a specified molecule based on a defined rms (root-mean-square) value. Conformers of all molecules were superposed according to the FIGO algorithm using a hyper template (HT) formed by rolipram and 5′-AMP in their bound conformation (**1q9m** and **1ptw**, respectively). One conformer per molecule was selected maximizing the intersection volume overlap between the superposed conformers and the HT.

FIGO alignment was carried out using MIFs from program Grid (O, N1, and C3 probes). The number of nodes (energy value) per molecule selected was equal to the number of its heavy atoms, N, except for the C3 probe (3N). These latter were selected so that the minimum distance between each node and the other was not less than 2 Å.

Docking. Docking calculation were performed using Glide program (FirstDiscovery v2.7, Schrödinger)[31] on a AMD Athlon 1800+ processor running Linux. All PDE4 crystal structures were prepared according to the protein preparation procedure recommended. Default input parameters were used in all computations (no scaling factor for the vdW radii of nonpolar protein atoms, 0.8 scaling factor for nonpolar ligand atoms). Upon completion of each docking calculation, three poses per ligand were saved. The best-docked structure was chosen using a model energy score (Emodel) derived from a combination of the Glide Score (Gscore, a modified and extended version of the empirically based ChemScore function[36]), Coulombic and the van der Waals energies, and the strain energy of the ligands.[31]

3D QSAR Analysis. Molecular Interaction Fields (MIFs) were computed with program Grid[2] using C3, DRY, N1, and O probes and the following parameters: 1 Å grid spacing, 22 × 23 × 27 (post-Glide model) and 29 × 27 × 31 (post-FIGO model) grid box dimension. The matrix derived from the unfolding of the probe−ligand interactions into vectors (one for each ligand considered) was submitted to Golpe[33] advanced pretreatment including max. cutoff = 0 kcal, zeroing = 0.01 kcal, min sd = 0.02 Å, N-level = 2, 3, and 4. The resulting variables were normalized according to the BUW procedure. The Smart Region Definition (post-Glide model: number of seed = 1545, critical distance cutoff = 1.0 Å, collapsing cutoff = 2.0 Å; post-FIGO model: number of seed = 2427, critical distance cutoff = 1.0 Å, collapsing cutoff = 2.0 Å) in combination with the Fractional Factorial Design was used in the variable selection. PCA based on the used probes was carried out: no outliers were found The optimal dimensionality of the PLS model was determined according to leave-one-out (LOO) and random groups (RG) cross-validation procedure. Predictive performance of the models was also obtained via external validation (q^2_{ext}) using the independent set of test compounds.

Acknowledgment. The Italian funding agency of MIUR (Ministero dell'Istruzione, dell'Università e della Ricerca) is thanked for financial support. The authors are grateful to Molecular Discovery (http://www.moldiscovery.com) for supplying the Grid and Volsurf software programs, free of charge, to the academic institution.

References

(1) Melani, F.; Gratteri, P.; Adamo, M.; Bonaccini, C. Field Interaction and Geometrical Overlap (FIGO): a new Simplex/experimental design-based computational procedure for superposing small ligand molecules. *J. Med. Chem.* **2003**, *46*, 1359−1371.

(2) (a) Goodford, P. J. A computational procedure for determining energetically favourable binding sites on biologically important macromolecules. *J. Med. Chem.* **1985**, *28*, 849−857. (b) Grid version 21 Molecular Discovery Ltd. 215 Marsh Road, 1st Floor HA5 5NE, Pinner, Middlesex, United Kingdom (http://www.moldiscovery.com).

(3) Duplantier, A. J.; Biggers, M. S.; Chambers, R. J.; Cheng, J. B.; Cooper, K.; Damon, D. B.; Eggler, J. F.; Kraus, K. G.; Marfat, A.; Masamune, H.; Pillar, J. S.; Shirley, J. T.; Umland, J. P.; Watson, J. W. Biarylcarboxylic acids and -amides: inhibition of phosphodiesterase type IV versus [^{3}H]rolipram binding activity and their relationship to emetic behavior in the ferret. *J. Med. Chem.* **1996**, *39*, 120−125.

(4) Masamune, H.; Cheng, J. B.; Cooper, K.; Eggler, J. F.; Marfat, A.; Marshall, S. C.; Shirley, J. T.; Tickner, J. E.; Umland, J. P.; Varquez, E. Discovery of microlmolar PDE IV inhibitors that exhibit much reduced affinity for the [^{3}H]-rolipram binding site: 3-norbornyloxy-4-methoxyphenylmethylene oxindoles. *Bioorg. Med. Chem. Lett.* **1995**, *5*, 1965−1968.

(5) Duplantier, A. J.; Andresen, C. J.; Cheng, J. B.; Cohan, V. L.; Decker, C.; DiCapua, F. M.; Kraus, K. G.; Johnson, K. J.; Turner, C. R.; Umland, J. P.; Watson, J. W.; Wester, R. T.; Williams, A. S.; Williams, J. A. 7-Oxo-4,5,6,7-tetrahydro-1*H*-pyrazolo[3,4-*c*]-pyridines as Novel Inhibitors of Human Eosinophil Phosphodiesterase. *J. Med. Chem.* **1998**, *41*, 2268−2277.

(6) Cheng J. B.; Cooper, K.; Duplantier, A. J.; Eggler, J. F.; Kraus, K. G.; Marshall, S. C.; Marfat, A.; Masamune, H.; Shirley, J. T.; Tickner, J. E.; Umland, J. P. Synthesis and in vitro profile of a novel series of cathecol benzimidazoles. The discovery of potent, selective phosphodiesterase type IV inhibitors with greatly attenuated affinity for the [^{3}H]Rolipram binding site. *Bioorg. Med. Chem. Lett.* **1995**, *5*, 1969−1972.

(7) Kleinman, E. F.; Campbell, E.; Giordano, L.; Cohan, V. L.; Jenkinson, T. H.; Cheng, J. B.; Shirley, J. T.; Pettipher, E. R.; Salter, E. D.; Hibbs, T. A.; DiCapua, F. M.; Bordner, J. Striking Effect of Hydroxamic Acid Substitution on the Phosphodiesterase Type 4 (PDE4) and TNF Inhibitory Activity of Two Series of Rolipram Analogues: Implications for a New Active Site Model of PDE4. *J. Med. Chem.* **1998**, *41*, 266−270.

(8) Christensen, S. B.; Guider, A.; Forstner, C. J.; Gleason, J. G.; Bender, P. E.; Karpinski, J. M.; DeWolf, W. E.; Barnette, M. S.; Underwood, D. C.; Griswold, D. E.; Cielinski, L. B.; Burman, M.; Bochonowicz, S.; Osborn, R. R.; Manning, C. D.; Grous, M.; Hillegas, L. H.; Bartus, J. O.; Ryan, M. D.; Eggleston, D. S.; Haltiwanger, R. C.; Torphy, T. J. 1,4-Cyclohexanecarboxylates: potent and selective inhibitors of phosophodiesterase 4 for the treatment of asthma. *J. Med. Chem.* **1998**, *41*, 821−835.

(9) Buckley, G. M.;Cooper, N.; Dyke, H. J.; Galleway, F.; Gowers, L.; Gregory, J. C.; Hannah, D. R.; Haughan, A. F.; Hellewell, P. G.; Kendall, H. J.; Lowe, C.; Maxey, R.; Montana, J. G.; Naylor, R.; Picken, C. L.; Runcie, K. A.; Sabin, V.; Tuladhar, B. R.; Warneck, J. B. H. 7-Methoxybenzofuran-4-carboxamides as PDE 4 Inhibitors: A Potential Treatment for Asthma. *Bioorg. Med. Chem. Lett.* **2000**, *10*, 2137−2140.

(10) Napoletano, M.; Norcini, G.; Pellacini, F.; Marchini, F.; Morazzoni, G.; Ferlenga, P.; Pradella, L. The synthesis and biological evaluation of a novel series of phthalazine PDE4 inhibitors I. *Bioorg. Med. Chem. Lett.* **2000**, *10*, 2235−2238.

(11) Napoletano, M.; Norcini, G.; Pellacini, F.; Marchini, F.; Morazzoni, G.; Ferlenga, P.; Pradella, L. Phthalazine PDE4 inhibitors. Part 2: the synthesis and biological evaluation of 6-methoxy-1,4-disubstituted derivatives. *Bioorg. Med. Chem. Lett.* **2001**, *11*, 33−37.

(12) Napoletano, M.; Norcini, G.; Pellacini, F.; Marchini, F.; Morazzoni, G.; Fattori, R.; Ferlenga, P.; Pradella, L. Phthalazine PDE4 inhibitors. Part 3: the synthesis and in vitro evaluation of derivatives with a hydrogen bond acceptor. *Bioorg. Med. Chem. Lett.* **2002**, *12*, 5−8.

(13) Burnouf, C.; Auclair, E.; Avenel, N.; Bertin, B.; Bigot, C.; Calvet, A.; Chan, K.; Durand, C.; Fasquelle, V.; Féru, F.; Gilbertsen, R.; Jacobelli, H.; Kebsi, A.; Lallier, E.; Maignel, J.; Martin, B.; Milano, S.; Ouagued, M.; Pascal, Y.; Pruniaux, M. P.; Puaud, J.; Rocher, M. N.; Terrasse, C.; Eriggleworth, R.; Doherty, A. M. Synthesis, structure−activity relationships, and pharmacological profile of 9-amino-4-oxo-1-phenyl-3,4,6,7-tetrahydro[1,4]-diazepino[6,7,1-*hi*]indoles: discovery of potent, selective phosphodiesterase type 4 inhibitors. *J. Med. Chem.* **2000**, *43*, 4850−4867.

(14) Buckley, G. M.;Cooper, N.; Davenport, R. J.; Dyke, H. J.; Galleway, F.; Gowers, L.; Haughan, A. F.; Hannah, D. R.; Lowe, C.; Montana, J. G.; Oxford, J.; Peake, J. C.; Picken, C. L.; Richard, M. D.; Sabin, V.; Sharpe, A.; Warneck, J. B. H. -Methoxyfuro[2,3-c]pyridine-4-carboxamides as PDE4 inhibitors: a potential treatment for asthma. *Bioorg. Med. Chem. Lett.* **2002**, *12*, 509−12.

(15) Buckley, G. M.; Cooperm N.; Dyke, H. J.; Galleway, F. P.; Gowers, L.; Haughan, A. F.; Kendall, H. J.; Lowe, C.; Maxey, R.; Montana, J. G.; Naylor, R.; Oxford, J.; Peake, J. C.; Picken, C. L.; Runcie, K. A.; Sabin, V.; Sharpe, A.; Warneck, J. B. 8-Methoxyquinoline-5-carboxamides as PDE4 inhibitors: a potential treatment for asthma. *Bioorg. Med. Chem. Lett.* **2002**, *12*, 1613−15.

(16) Billah, M.; Buckley, G. M.; Cooper, N.; Dyke, H. J.; Egan, R.; Ganguly, A.; Gowers, L.; Haughan, A. F.; Kendall, H. J.; Lowe, C.; Minnicozzi, M.; Montana, J. G.; Oxford, J.; Peake, J. C.;

Picken, C. L.; Piwinski, J. J.; Naylor, R.; Sabin, V.; Shih, N. Y.; Warneck, J. B. 8-Methoxyquinolines as PDE4 inhibitors. *Bioorg. Med. Chem. Lett.* **2002**, *12*, 1617−1619.
(17) Pascal, Y.; Andrianjara, C. R.; Auclair, E.; Avenel, N.; Bertin, B.; Calvet, A.; Féru, F.; Lardon, S.; Moodley, I.; Ouagued, M.; Payne, A.; Pruniaux, M. P.; Szilagyi, C. Synthesis and structure−activity relationships of 4-oxo-1-phenyl-3,4,6,7-tetrahydro-[1,4]-diazepino[6,7,1-hi]indoles: novel PDE4 inhibitors. *Bioorg. Med. Chem. Lett.* **2000**, *10*, 35−38.
(18) Essayan, D. M. Cyclic nucleotide phosphodiesterase. *J. Allergy Clin. Immunol.* **2001**, *108*, 671−80.
(19) Burnouf, C.; Pruniaux, M. P. Recent advances in PDE4 inhibitors as immunoregulators and anti-inflammatory drugs. *Curr. Pharm. Des.* **2002**, *8*, 1255−96.
(20) Xu, R. X.; Hassel, A. M.; Vanderwall, D.; Lambert, M. H.; Holmes, W. D.; Luther, M. A.; Rocque, W. J.; Milburn, M. V.; Zhao, Y.; Ke, H.; Nolte, R. T. Atomic structure of PDE4: insights into phosphodiesterase mechanism and specificity. *Science* **2000**, *288*, 1822−25.
(21) Berman, H. M.; Westbrook, J.; Feng, Z.; Gilliland, G.; Bhat, T. N.; Weissig, H.; Shindyalov, I. N.; Bourne, P. E. The Protein Data Bank. *Nucleic Acids Res.* **2000**, *28*, 235−242.
(22) Lee, M. E.; Markowitz, J.; Lee, J.-O.; Lee, H. Crystal structure of phosphodiesterase 4D and inhibitor complex. *FEBS Lett.* **2002**, *530*, 53−58.
(23) Huai, Q.; Wang, H.; Sun, Y.; Kim, H.-Y.; Liu, Y.; Ke, H. Three-dimensional structures of PDE4D in complex with roliprams and implication on inhibitor selectivity. *Structure* **2003**, *11*, 865−873.
(24) Huai, Q.; Colicelli, J.; Ke, H. The crystal structure of AMP-bound PDE4 suggests a mechanism for phosphodiesterase catalysis. *Biochemistry* **2003**, *42*, 13220−13226.
(25) Huai, Q.; Liu, Y.; Francis, S. H.; Corbin, J. D.; Ke, H. Crystal structures of phosphodiesterases 4 and 5 in complex with inhibitor 3-isobutyl-1-methylxanthine suggest a conformation determinant of inhibitor selectivity. *J. Biol. Chem.* **2004**, *279*, 13095−13101.
(26) Davis, A.; Warrington, B. H.; Vinter, J. G. Strategic approach to drug design. II. Modelling studies on phosphodiesterase substrates and inhibitors. *J. Comput.-Aided Mol. Des.* **1987**, *1*, 97−120.
(27) Marivet, M. C.; Bourguignon J. J.; Lugnier, C.; Mann, A.; Stoclet, J. C.; Wermutht C. G. Inhibition of Cyclic Adenosine-3′,5′-monophosphate Phosphodiesterase from Vascular Smooth Muscle by Rolipram Analogues. *J. Med. Chem*. **1989**, *32*, 1450−1457.
(28) Xu, R. X.; Rocque, W. J.; Lambert, M. H.; Vanderwall, D. E.; Luther, M. A.; Nolte, R. T. Crystal structures of the catalytic domain of phosphodiesterase 4B complexed with AMP, 8-Br-AMP, and rolipram. *J. Mol. Biol.* **2004**, *337*, 355−365.
(29) Percival, M. D.; Yeh, B.; Falgueyret, J. P. Zinc dependent activation of cAMP-specific phosphodiesterase (PDE4A). *Biochem. Biophys. Res. Commun.* **1997**, *241*, 175−180.
(30) Callahan, S. M.; Cornell, N. W.; Dunlap P. V. Purification and properties of periplasmic 3′: 5′-cyclic nucleotide phosphodiesterase. A novel zinc-containing enzyme from the marine symbiotic bacterium Vibrio fischeri. *J. Biol. Chem.* **1995**, *270*, 17627−17632.
(31) (a) Friesner, R. A.; Banks, J. L.; Murphy, R. B.; Halgren, T. A.; Klicic, J.; Mainz, D. T.; Repasky, M. P.; Knoll, E. H.; Shelley, M.; Perry, J. K.; Shaw, D. E.; Francis P.; Shenkin P. S. Glide: A New Approach for Rapid, Accurate Docking and Scoring. 1. Method and Assessment of Docking Accuracy. *J. Med. Chem.* **2004**, *47*, 1739−1749. (b) Schrödinger. L. L. C., New York (http://www.schrodinger.com).
(32) Scapin, G.; Patel, S. B.; Chung, C.; Varnerin, J. P.; Edmondson, S. D.; Mastracchio, A.; Parmee, E. R.; Singh, S. B.; Becker, J. W.; Van der Ploeg, L. H.; Tota, M. R. Crystal structure of human phosphodiesterase 3B: atomic basis for substrate and inhibitor specificity. *Biochemistry* **2004**, *43*, 6091−6100.
(33) GOLPE 4.5. Multivariate Infometric Analysis Srl. (http://www.miasrl.com).
(34) InsightII 2000, Accelrys Inc. (http://www.accelrys.com).
(35) (a) Volsurf v.3.0.11. (b) Crivori, P.; Cruciani, G.; Carrupt, P.-A.; Testa, B. Predicting Blood-Brain Barrier Permeation from Three-Dimensional Molecular Structure. *J. Med. Chem.* **2000**, *43*, 2204−2216.
(36) Jorgensen, W. L.; Maxwell, D. S.; Tirado-Rives, J. Development and Testing of the Opls All Atom Force Field on Conformational Energetics and Properties of Organic Liquids. *J. Am. Chem. Soc.* **1996**, *118*, 11225−11236.

JM049289B